Atmos. Chem. Phys. Discuss., 6, 5671–5709, 2006
www.atmos-chem-phys-discuss.net/6/5671/2006/

Atmospheric Chemistry and Physics Discussions

Hemispheric ozone variability indices derived from satellite observations and as diagnostics for coupled chemistry-climate models

T. Erbertseder[1], V. Eyring[2], M. Bittner[1], M. Dameris[2], and V. Grewe[2]

[1]German Remote Sensing Data Center, DFD, German Aerospace Center, DLR, Germany
[2]Institute for Atmospheric Physics, German Aerospace Center, DLR, Germany

Received: 4 April 2006 – Accepted: 24 May 2006 – Published: 30 June 2006

Correspondence to: T. Erbertseder (thilo.erbertseder@dlr.de)

Abstract

Dynamics and chemistry of the lower and middle stratosphere are characterized by manifold processes on different scales in time and space. The total column density of ozone, measured by numerous instruments, can be used to trace the resulting variability. In particular, satellite-borne spectrometers allow global observation of the total ozone distribution with proven accuracy and high temporal and spatial resolution. In order to analyse the zonal and hemispherical ozone variability a spectral statistical Harmonic Analysis is applied to multi-year total ozone observations from the Total Ozone Monitoring Spectrometer (TOMS). As diagnostic variables we introduce the hemispheric ozone variability indices one and two. They are defined as the hemispheric means of the amplitudes of the zonal waves number one and two, respectively, as traced by the total ozone field.

In order to demonstrate the capability of the diagnostic for intercomparison studies we apply the hemispheric ozone variability indices to evaluate total ozone fields of the coupled chemistry-climate model ECHAM4.L39(DLR)/CHEM (hereafter: E39/C) against satellite observations. Results of a multi-year model simulation representing "2000" climate conditions with an updated version of E39/C and corresponding total ozone data of TOMS from 1996 to 2004 (Version 8.0) are used. It is quantified to what extent E39/C is able to reproduce the zonal and hemispherical large scale total ozone variations. The different representations of the hemispheric ozone variability indices are discussed.

Summarizing the main differences of model and reference observations, we show that both indices, one and two, in E39/C are preferably too high in the Northern Hemisphere and preferably too low in the Southern Hemisphere. In the Northern Hemisphere, where the coincidence is generally better, E39/C produces a too strong planetary wave one activity in winter and spring as well as a too high interannual variability.

For the Southern Hemisphere we conclude that model and observations differ significantly during the ozone hole season. In October and November amplitudes of wave

ACPD

6, 5671–5709, 2006

number one and two are underestimated. This explains that E39/C exhibits a too stable polar vortex and a too low interannual variability of the ozone hole. Further, a strong negative bias of wave number one amplitudes in the tropics and subtropics from October to December is identified, which may also contribute to the zonal-symmetric polar vortex. The lack of wave two variability in October and November leads to weak vortex elongation and eventually a too late final warming. Contrary, too high wave number two amplitudes in July and August indicate why the polar vortex is formed too late in season by E39/C.

In general, the hemispheric ozone variability indices can be regarded as a simple and robust approach to quantify differences in total ozone variability on a monthly mean basis. Therefore, the diagnostic represents a core diagnostic for model intercomparisons within the CCM Validation Activity for WCRP's (World Climate Research Programme) SPARC (Stratospheric Processes and their Role in Climate) regarding stratospheric dynamics.

1 Introduction

Ozone is well known to play a major role in understanding the atmosphere. Quantifying its distribution and variability over a wide range of scales both temporal and spatial, has therefore been an intense subject of scientific research. With the advent of satellite borne instruments in the 70's, global observations of total column ozone have been performed on a routine basis.

Observations of the Total Ozone Monitoring Spectrometer (TOMS) since November 1978 have been enabled to study the morphology, depth and evolution of the Antarctic ozone hole (Stolarski et al., 1986; Newman et al., 1986; Schoeberl et al., 1986) and the occurrence and size of low ozone events at mid-latitudes (James, 1998; Bojkov and Balis, 2001). Together with other satellite borne instruments (BUV and SBUV (Solar Backscatter UV), TOVS and ATOVS (Advanced TIROS Operational Vertical Sounder), GOME (Global Ozone Monitoring Experiment), SCIAMACHY (Scanning Imaging Ab-

sorption Spectrometer for Atmospheric Cartography), OMI (Ozone Monitoring Instrument)) and the ground-based network, a continuous global monitoring of total column ozone and its trends with special attention to polar and mid-latitude levels is possible (IPCC, 2001; WMO, 2003). Today there is broad agreement that in order to detect signs of ozone recovery (e.g. Newchurch et al., 2003; Steinbrecht et al., 2004; Yang et al., 2005; Huck et al., 2005; Hadjinicolaou et al., 2005; Dameris et al., 2005, 2006) a continuous monitoring of the ozone layer as well as a good understanding of the underlying processes that govern ozone variability is needed (WMO, 2003).

Considerable work has been performed to study relationships between total ozone column and atmospheric dynamics and chemistry. For example early studies to correlate the ozone total column ozone with weather systems were made as early as by Dobson (1926) and by Reed (1950). Ozone variability exhibits signals due to a large variety of processes induced by the 11-year solar cycle (e.g. Haigh, 1996; Zerefos et al., 1997; Labitzke et al., 2002), the Quasi Biennial Oscillation (e.g. Bojkov and Fioletov, 1995; Steinbrecht, 2001), the El Nino Southern Oscillation (e.g. Kayano, 1997), Northern Atlantic Oscillation (e.g. Schnadt and Dameris, 2003; Appenzeller et al., 2000), Arctic Oscillation (e.g. Nikulin and Repinskaya, 2001), volcanic eruptions (e.g. Robock, 2000) or trends related to the increase of anthropogenic emissions like stratospheric halogen compounds since the 1970s (WMO, 2003). The latter constitutes the significant influence of chemistry. Another part of the observed ozone variability can be attributed to meteorological conditions and phenomena like jet streams (e.g. Shapiro et al., 1982), anticyclones and blocking high pressure systems (Reiter and Gao, 1982; Dameris et al., 1995), cyclogenesis and cut-off lows (Thomas et al., 2003). The impact of these factors on the total ozone variations was recently quantified by Steinbrecht et al. (2003) by a multi-linear regression analysis using TOMS data.

It has been shown that total column ozone can be considered as a tracer for stratospheric dynamics. Especially, planetary waves were found to substantially contribute to total ozone variability (Wirth, 1993). This is because its chemical lifetime in the lower and middle stratosphere, where approximately over 90% of the vertical ozone abun-

dance is found, is long enough to trace transport processes (e.g. Wirth, 1993). In turn, ozone revealed itself as an excellent parameter to characterise wave induced variability of the stratosphere. The focus of this work is on planetary-scale waves.

Planetary-scale waves are frequently observed in the middle atmosphere (stratosphere and mesosphere). In their simplest form of Rossby-waves they occur due to the variation of the Coriolis parameter with latitude (e.g. Andrews et al., 1987). They show up as transient waves with periods of several days to a few weeks while excitation and decay occurs on time scales of 1–2 months (Salby, 1984). Some of these large-scale waves are forced by features at the surface, by orography and thermal contrast, e.g. between land and sea. In that case they are (quasi-) stationary with respect to the surface to produce, for example, the Aleutian anticyclone. There are several reasons that constitute the substantial interest in these phenomena. Planetary waves drive the circulation away from radiative equilibrium. They are known to be an important source mechanism for transport processes in the stratosphere, are responsible for the intermittent mid-winter breakdown of the polar vortices called sudden stratospheric warmings and are involved in vortex erosion processes (e.g. Schoeberl and Hartmann, 1991). Especially, the latter point is of substantial interest since the significant springtime depletion of ozone in polar regions require that polar stratospheric air has a high degree of dynamical isolation and extremely low temperatures necessary for the formation of polar stratospheric clouds (e.g. Turco et al., 1989). The strength of planetary waves can be characterized by their amplitude. Based on total column ozone as a tracer, the amplitude of the quasi-stationary waves can be derived from satellite observations on a daily basis (Bittner et al., 1997). Since total ozone is considered, this quantity comprises the coupled dynamical and chemical variability and can therefore be used as a proxy to quantify the accuracy of numerical models describing the dynamics and chemistry of the stratosphere.

Satellite and ground-based instruments allow the continuous monitoring of ozone variations and to improve the understanding of the underlying processes. Coupled chemistry-climate models (CCMs) with detailed descriptions of the stratosphere can

address how climate change, stratospheric ozone and UV radiation interact, now and in the future (Austin et al., 2003; WMO, 2003). Therefore, these models provide fundamental information for ozone, UV and climate assessments (SPARC, 1998; WMO, 2003; IPCC, 2001; IPCC/TEAP, 2005).

As mentioned above, the stratosphere and its key constituent ozone are strongly influenced by manifold dynamical and chemical processes, which have to be realistically represented in CCMs (Eyring et al., 2005). One key process is the forcing and propagation of planetary-scale waves. Multi-year satellite observations of total ozone, as derived from the Total Ozone Monitoring Spectrometer (TOMS) offer a consistent source for the evaluation of model results, since they provide information about ozone variability with proven accuracy and considerable temporal and spatial resolutions. Based on an episode of the TOMS total ozone record zonal and hemispheric variability diagnostics are applied and compared to the results of the CCM E39/C in order to check the model's ability to reproduce it correctly.

The temporal and spatial variability of the hemispheric diagnostic variables are addressed and their suitability for comparison studies is discussed.

The paper is structured as follows: Sect. 2 gives an overview on the satellite observations and the model simulation used in this analysis. The spectral statistical approach that has been developed to derive zonal amplitudes from total ozone fields is described in Sect. 3. Section 4 summarizes results on total ozone variability and hemispheric ozone variability indices. We end with a conclusion.

2 Data

2.1 Satellite observations

In order to analyse the hemispheric and zonal ozone variability and the ability of the CCM to reproduce this variability we consider backscatter measurements of the Total Ozone Monitoring Spectrometer (TOMS) having been operated on different platforms

since 1978 (McPeters et al., 1998).

TOMS samples backscattered ultraviolet radiation at six wavelengths and provides a continuous mapping of total column ozone. It provides almost complete daily global coverage of ozone outside the polar night region. We apply TOMS data in the most recent version 8.0 (Bhartia and Wellemeyer, 2004), thus TOMS on METEOR-3 is not used.

TOMS V8 uses only two wavelengths (317.5 and 331.2 nm) to derive total ozone while other 4 wavelengths (depending on the instrument version) are used for diagnostics and error corrections. The algorithm improvements include an aerosol/glint correction based on the aerosol index, new climatologies for ozone profiles, temperature profiles and tropospheric ozone, an improved surface reflectivity model and a more accurate radiative transfer calculation in the forward model. The algorithm is capable of producing total ozone with a random-mean-square error of about 2%. The errors, however, typically increase with solar zenith angle and in presence of heavy aerosol loading (Bhartia and Wellemayer, 2004).

TOMS observations give an excellent and representative data record to study the zonal ozone variability and to evaluate model results. Since the focus of the study is on amplitudes, not absolute values or trends, the results are not influenced by instrument degradation.

2.2 Model description and design of model simulations

E39/C is a coupled chemistry-climate model (CCM) which has been used for different studies regarding past and future atmospheric composition and has been compared to observations (Hein et al., 2001; Schnadt et al., 2002; Eyring et al., 2003; Dameris et al., 2005; Steinbrecht et al., 2006). The model has been participating in a detailed assessment of CCMs of the stratosphere (Austin et al., 2003). For this study, a horizontal resolution of T30 and a corresponding Gaussian transform latitude-longitude grid of $3.75^\circ \times 3.75^\circ$ is employed, on which model physics, chemistry, and tracer transport are calculated. In the vertical the model has 39 layers extending from the surface

to the top centred at 10 hPa (Land et al., 2002). The chemistry model CHEM (Steil et al., 1998) is based on the family concept. It includes the most important gaseous and heterogeneous reactions to simulate upper tropospheric and lower stratospheric ozone chemistry.

A time-slice experiment, which in contrast to a transient model simulation is performed with fixed boundary conditions for a specific year, has been carried out under "2000" conditions for this study. An improved model version has been employed. The improvements include photolysis at solar zenith angles higher than 87.5° (Lamago et al., 2003) and new reaction rates for heterogeneous and homogeneous reactions (Sander et al., 2000). A detailed description of the updated model version is given in Dameris et al. (2005).

Mixing ratios for well-mixed greenhouse gases (CO_2, N_2O, CH_4) for the 2000 time-slice simulation are prescribed according to observations (IPCC, 2001). The upper boundary values for Cl_x, NO_y, and zonal chlorofluorocarbon (CFC) fields are taken from a transient model simulation of the Mainz 2-D model, adapted to observations (WMO, 1999). Anthropogenic as well as natural emissions of nitrogen oxides (NO_x=NO+NO_2) are also considered. Table 1 summarizes mixing ratios of greenhouse gases and different NO_x emissions from anthropogenic and natural sources. Sea surface temperatures (SSTs) are prescribed as monthly mean values following the global sea ice and sea surface temperature (HadISST1) data set provided by the UK Met Office Hadley Centre (Rayner et al., 2003). The data are averaged over the years 1995 to 1998.

3 Method

3.1 Harmonic Analysis

In order to quantify the zonal variability in total ozone we apply a spectral statistical Harmonic Analysis approach to monthly means of TOMS total ozone observations and the vertically integrated ozone fields of E39/C. To allow a comparison to the model

ACPD
6, 5671–5709, 2006

results, the satellite observations were regridded to the spatial discretisation T30 of E39/C which equals a longitude-latitude grid of 3.75°×3.75° mesh size.

The applied analysis technique was developed on the basis of Bittner et al. (1994) and makes use of the concept of the deconvolution of the power spectrum at selected latitudes to produce amplitudes and phases for individual longitudinal sinusoidals. A power spectrum is calculated and the dominating spectral feature (phase and amplitude) is determined. A sinusoid to that spectral feature is fitted to the data (Eq. 1) by means of least squares (Eq. 2). The residuals are computed and a second trigonometric function is fitted to the residuals. This procedure is repeated for all harmonics (eight in this case). Additionally, with each step all previous determined spectral components are fitted again, iteratively. This is because the resulting linear combination of sinusoids turns out not to be unimodal when fitting the data. In other words, the variance of the data series can be reduced if the current and the former sinusoidals are varied simultaneously. Bittner et al. (1994) have shown that this "all step mode" allows one to find a much better parameter vector for the least squares scheme than a "one step mode". The sinoid can be denoted as

$$\hat{y}_{ik} = \sum_{j=1}^{n} A_{ij} \sin\left(\omega_{ij}\lambda_{ik} - \varphi_{ij}\right), \tag{1}$$

where $\hat{y}_{ik}$ represents the k-th total column ozone value as derived from TOMS or E39/C within the i-th latitude segment, n denotes the number of sinusoidals used, A_{ij} is the amplitude of the j-th oscillation within the i-th latitude segment, and ω_{ij} denotes the angular frequency of the j-th oscillation. λ_{ik} stands for the longitude at the k-th measurement value in the i-th latitude segment and φ_{ij} represents the phase of the i-th oscillation for latitude segment i.

The best fit is determined by the condition

$$\sum_{i=1}^{m}\sum_{j=1}^{n}\left(\hat{y}_{ij} - y_{ij}\right)^2 \quad \Rightarrow \quad \min. \tag{2}$$

The Harmonic Analysis approach accounts for about 98% of the variance of the data when superimposing eight harmonics. However, since in this case 24 free parameters have to be estimated by a set of nonlinear equations, converging problem have to be overcome. Therefore, the Newton-Raphson solver for nonlinear systems of equations is applied (Ortega and Rheinboldt, 1970).

For physical reasons some constraints are evident. The fitted zonal sinusoidal functions are well suited, as mentioned before, to describe the global circulation pattern of the lower and middle stratosphere by modelling the zonal structure of such waves (e.g. Barnett and Labitzke, 1990). This point, however, defines a constraint for the Harmonic Analysis of total ozone data because planetary waves are global phenomena, which means that the wavelengths must be the same at all latitudes while amplitudes and phases are allowed to vary.

The Harmonic Analysis shows significant improvements compared to a Fourier-Analysis, which can cause leakage and anti-aliasing effects and is, mathematically speaking, strictly defined for endless data series only.

3.2 Hemispheric ozone variability index

Total column ozone fields are used to trace the resulting variability due to dynamical and chemical processes in the stratosphere. In order to quantify zonal total ozone variability, the amplitudes of the zonal wave number one and two are derived as a function of latitude. As a diagnostic variable we introduce hemispheric ozone variability indices number one and two. They are defined as the hemispheric mean amplitudes of the zonal waves number one and two, respectively, as traced by the total ozone field and derived by the Harmonic Analysis (Sect. 3.1). Notwithstanding the fact that the zonal waves in total column ozone can be interpreted as a manifestation of the quasi-stationary planetary waves, there is a contribution of chemical processes. Most significant in this respect is ozone depletion in the polar vortices or long term changes due to an increase of ozone depleting substances as observed e.g. in the mid-latitudes. However, this does not affect the main subject of this study which is to analyse results

from satellite data with model simulations. The diagnostic variables account for variability caused by coupled dynamic and chemical processes, a CCM should be able to reproduce.

The diagnostic is applied to multi-year TOMS total ozone data first. Since the indices give a simple hemispheric measure of coupled dynamical and chemical ozone variability, it is subsequently used for the evaluation of CCM E39/C results of total column ozone.

4 Results

4.1 TOMS

4.1.1 Time series of hemispheric ozone variability index 1 (1978 to 2004)

Figure 1 shows time series of the monthly means of the ozone variability index one for the Northern (top) and Southern Hemisphere (bottom). It is derived from all TOMS observations (V 8.0) from November 1978 to April 1993 and from July 1996 to December 2004. The dominant feature of the time series is a pronounced annual cycle. Yearly maxima from 20 to 40 Dobson Units are found during winter, minima of 5 to 8 DU occur during summer. Note, that there is a clear anticorrelation in wave activity between the hemispheres. This is interpreted as a lack of planetary wave activity during the summer months, when the mean stratospheric flow is easterly and therefore prevents planetary waves from vertical propagation into the stratosphere. This is consistent with the findings first obtained by Charney and Drazin (1961). Enhanced wave one activity, however, can be identified in the Northern Hemisphere, at least occasionally during summer months. These signatures cannot be explained with the abovementioned theory of planetary waves propagating from the troposphere into the lower stratosphere. In the Southern Hemisphere the largest indices are found during austral spring. This is associated to an off-pole displacement of the polar vortex and reflects partly increased

amplitudes in the zonal ozone field due to reduced ozone levels inside the vortex.

4.1.2 Interannual variability of hemispheric ozone variability index 1 and 2 (1978 to 2004)

The interannual mean and standard deviation of the hemispheric ozone variability indices one and two for both hemispheres and each month is shown in Fig. 2. Again, the results are derived for all available TOMS total ozone observations (Version 8) between November 1978 and October 2004. Both indices show a characteristic annual cycle for each hemisphere. In the Northern Hemisphere the observed maximum of 24 DU can be found in February, the minimum of 7 DU in June. This reflects the peaking dynamic activity in late winter and the discontinued upward propagation of tropospheric waves in summer. Consequently, the standard deviation of the index for the Northern Hemisphere is highest in February and lowest from June to September.

In the Southern Hemisphere the minimum can be found in January (7 DU) and the maximum in October (27 DU). Compared to a more sinusoidal annual cycle in the Northern Hemisphere, we observe a sharp decrease from October to low values in December, which can be associated to the breakdown of the polar vortex. The annual cycle of the standard deviation is very similar to that of the Northern Hemisphere considering the season. However, high interannual variability is extended into spring and shows a maximum during October. The maxima in October of both, mean and standard deviation, results from the off-pole displacement of the polar vortex leading to large zonal amplitudes of wave number one in the ozone field and will be discussed later.

The annual cycles of the hemispheric ozone variability index two follows the behaviour of variability index one to some extent. In the Northern Hemisphere, the maximum of 12 DU is found in February, the yearly minimum of 5 DU occurs in August. The interannual variability is highest in winter including March. In the Southern Hemisphere the ozone variability index two shows a relatively smooth behaviour. Both mean and standard deviation are lowest from January to April and increase peaking in Octo-

ber. This behaviour coincides with the hemispheric variability index one. The largest standard deviation in October mirrors the elongation of the polar vortex.

4.2 Comparison of TOMS and E39/C

In order to demonstrate the capability of the new diagnostic for evaluation studies we apply the diagnostic variables in the following to compare satellite observations with results of a time slice experiment of E39/C. The time slice experiment results comprise of 20 years representative for the atmospheric conditions of the year 2000 (hereafter: E2000). Since the "years" of the time slice experiment do not represent the same chronological order as in the atmosphere as observed by TOMS, no single years can be compared directly. Instead, the experiment has the advantage to give different realisations of the same year and thus, the focus of this study is on interannual means and variability. In order to provide adequate atmospheric observations for the year 2000 simulation, TOMS data between November 1996 and October 2004 (hereafter: T2000) are considered. These eight years sufficiently reflect perturbed stratospheric chemistry and polar vortex dynamics around the year 2000.

Although T2000 consists of 8 years only, which is a short period on climatological time scales, it can be shown that this period gives a mean representation of the ozone variability on a hemispheric scale. Not only for the Southern, but also for the Northern Hemisphere the hemispheric indices are comparable when two different periods are considered (1978 to 2004 in Fig. 2 and 1996 to 2004 in Figs. 6 and 8). The hemispheric indices are thus robust parameters that reflect the mean hemispheric state and standard deviation. As can be inferred from Fig. 1 it is not sensitive to, statistically spoken, outliers like the polar vortex split in September 2002.

4.2.1 Total ozone zonal means

Since the diagnostic is based on total ozone we start by discussing zonal means of total ozone and their variability. Figure 3 (top) shows a comparison of total ozone

zonal means and standard deviations for T2000 and E2000. Results are presented for the selected months January, April, July and October. These months are chosen to represent typical seasonal conditions, which gives a clearer picture than seasonal means. The corresponding relative differences for mean and standard deviation (Fig. 3, bottom) also depict the statistical significance at the 95% level.

The zonal means of T2000 show the well known features and seasonal variability of total ozone. While the amounts are nearly constant in the tropics (around 240 to 260 DU), recognizable also by the low standard deviations, high levels occur at northern mid and high latitudes in winter and spring (January and April). The massive depletion of stratospheric ozone in austral spring results in strongly reduced ozone columns in October at southern polar latitudes. Here a total column reduction below 220 DU indicates ozone hole conditions.

When comparing T2000 and E2000 zonal means of total ozone throughout all seasons a good latitudinal coincidence of the shape of the statistical moments can be found. Worth mentioning is the latitudinal coincidence of the mid-latitude ozone maximum in both hemispheres. As the only exception the ozone maximum between 50° S to 60° is shifted equatorwards in E39/C (up to 10° in April). This can be attributed to an equatorward displacement of the summer vortex, which was also identified in the zonal winds of a transient run of E39/C (Dameris et al., 2005).

Contrary to the structural agreement a positive bias of E39/C is evident in all months with maxima up to 20% north of 20° N (Fig. 3, bottom). The largest absolute positive bias is found north of 40° N with 60 DU. The bias is smallest in southern polar latitudes (<50° S). There is no significant difference in the total ozone zonal means south of 50° S in January, July and October. Notably, the Antarctic ozone hole levels are well met, which indicates that heterogeneous chemistry is sufficiently represented. This model improvement can partly be attributed to the introduction of large solar zenith angles that are now taken into account for the calculation of photolysis rates (Lamago et al., 2003).

Figure 3 further reveals that E2000 generally underestimates the standard deviation,

which stands for the zonal variability. Positive exceptions are associated with the north hemispheric mid-latitude ozone maximum in July and latitudes south of 40° S in January and April. The highest positive bias in the standard deviation occurs in southern polar latitudes in January. This is related to the persistent polar vortex in E39/C and will be resumed later in more detail.

When analysing zonal means of total ozone, it has to be stressed that 8 years are too short a period to quantify a significant climatological zonal mean state, especially for the Northern Hemisphere and its sequence of warm and cold winters. However, we are not aiming at a trend analysis and concentrate on evaluating the general deviations on a zonal and hemispherical scale. Although E2000 consists of 20 years the model mainly tends to underestimate the zonal standard deviation compared to T2000. Further, the peculiarity of the vortex split in austral spring 2002 does not show up as increased standard deviation or difference (September not shown here).

To give a more general picture of the models ability to reproduce total ozone budgets and to increase statistical significance compared to zonal means the findings from above (Fig. 3) are summarized in a hemispheric diagnostic. Area weighted zonal mean values are averaged for each hemisphere. Figure 4 shows the hemispheric total ozone means for each month of E2000 and T2000 (top) as well as the corresponding relative differences (bottom). In both hemispheres the mean annual cycle is well reproduced by E39/C. However, a positive bias in E2000 is evident for both hemispheres and all months. For the Northern Hemisphere the relative difference is largest in December (18.2%) and smallest in June (12.8%). Largest differences for the Southern Hemisphere occur in May (11.4%) and smallest in November (5.5%). This coincides with the results of Hein et al. (2001) and Schnadt et al. (2002). Thus, it can be concluded that none of the model improvements described in Sect. 2.2 has reduced the positive total ozone bias. Recent studies further confirm that the bias is not related to the uppermost model level of E39/C centred at 10 hPa and an insufficient residual circulation. The positive bias is still evident in MA-ECHAM/CHEM with a top level at 0.1 hPa (Steil et al., 2003; Steinbrecht et al., 2006).

4.2.2 Zonal amplitudes of wave one

In order to analyse the variability in E2000 and T2000, the amplitude of the zonal wave number one in total ozone is derived as a function of latitude (Fig. 5).

First we focus on the results for T2000 as reference. In the Northern Hemisphere high amplitudes dominate in winter and spring, low ones during summer and autumn. Maxima are found between about 60° and 70° N. In general, there is a decrease in zonal amplitude towards the tropics. Two local minima can be identified. One can be found throughout the year at 30° N–40° N, which could be associated, the subtropical transport barrier. Another pronounced minimum is detected at 10° N in winter, shifting to 20° N in summer and moving back again southwards from October on. This feature is attributed to effects related to the ITCZ. Within the minimum the amplitudes of wave one are reduced nearly to zero. This corresponds to the area of low total ozone variability in the tropics. When total ozone is considered high amplitudes are not only due to strong planetary wave activity, but also due to accumulation of ozone during polar night, low solar zenith angles and advection.

The variability traced by the amplitude of wave number one in the Southern Hemisphere is dominated by processes related to the polar vortex. Massive ozone depletion and off-pole displacements of the polar vortex result in large amplitudes peaking in October (90 DU). The mean development of the polar vortex (and the associated Antarctic ozone hole) and its interannual variability from August to December are clearly identifiable.

A subtropical minimum can be identified at about 30° S from January to March which shifts northwards to 15° S until August and then moves back. No counterpart, however, can be identified for the second local minimum (see above).

In the following we outline the relative differences of the T2000 wave number one amplitudes with respect to E2000. When comparing E2000 to T2000 the coincidence of both, mean and standard deviation, is especially strong from April to December for latitudes north of 50° N where no significant differences can be found. However, for the

Northern Hemisphere large deviations can be identified in February and March north of 60° N, where E2000 exceeds T2000 up to 150%. Systematic deviations for a few months further occur between 40° N and 50° N. These findings reflect the problems associated with the applied semi-Lagrange transport scheme resulting in a smoothing of gradients (Grewe et al., 2002). In particular, the transport barriers are formed too weak and ozone is transported (dispersed) southwards into the mid-latitudes too fast.

However, the two local minima over the Northern Hemisphere in the tropics and subtropics already discussed above can be identified in E2000 data as well. The coincidence of these smaller scale structures is good in all months except for July and August. Then, E39/C underestimates the amplitudes between 20° N and 45° N by 50% so that the local maximum at 35° N is not as pronounced as in T2000. From September to December the minima are not as pronounced as in E2000. Explicitly, the amplitudes between 10° N and 25° N are significantly overestimated in E2000 in January, February, June and October to December. It has to be emphasised, however, that small shifts of a relative maximum/minimum in meridional direction can result in large relative differences.

The most striking differences for wave one can be found during southern hemispheric spring associated with the evolution and persistence of the polar vortex. While the amplitudes south of 50° S are significantly underestimated from May to November, they are overestimated in December and January up to 120%. The comparison shows, that the modelled polar vortex and the ozone hole are too persistent, the final break down occurs about one month too late. This is in agreement with the results of Hein et al. (2001) and Schnadt et al. (2002). The reason for that can be given here: as the amplitudes of wave one are underestimated by E39/C in September and October and the wave forcing is too weak it can be followed that the interannual variability of the ozone hole is too low and that the polar vortex is too stable in terms of off-pole displacements which would result in large zonal amplitudes in the total ozone field. Contrary to the too low amplitudes south of 50° S from May to November, we identify a significant overestimation at 25° S in August and September which results in a smoothing of gradients. A

further new result related to Southern Hemisphere variability is that E39/C underestimates the wave one amplitude from October to December south of 50° S by 20 to 70%. The mean and interannual variability during ozone hole conditions are reasonably meet and the ozone hole season in E39/C shows a time lag of approximately three weeks (Lamago et al., 2003). Taking into account this fact, the deviations of the statistical moments are expected to be smaller. This can be regarded as a general problem when comparing CCM results with observations. To demonstrate the differences associated with a temporal shift in season we show all month here.

For both data sets a similar behaviour as a function of latitude can be observed. Distinct differences, however, are evident.

It has to be stressed again that the wave amplitudes in the total ozone fields are not only influenced by dynamical processes but also by chemical processes depending on latitude and season. We can infer from Fig. 5 that the conclusions are very heterogeneous and partly difficult to interpret, especially when multi-model comparisons are carried out. Therefore, we propose a hemispheric diagnostic in this study that allows a more generalised view.

4.2.3 Hemispheric ozone variability index one

As already shown in Figs. 1 and 2, the hemispheric ozone variability index one shows a pronounced annual cycle for each hemisphere. Figure 6 depicts the ozone variability index one for the Northern and Southern Hemisphere derived from T2000 and E2000 respectively, and the corresponding differences (bottom). Before addressing coincidences and differences, we first outline the results for T2000. The index one mirrors the annual cycles of hemispherical averaged zonal variability. In the Northern Hemisphere the observed maximum of 23 DU can be found in February, the minimum of 7 DU in June. This reflects the peaking dynamic activity in spring and the discontinued upward propagation of tropospheric waves in summer. The seasonal cycle is different in the Southern Hemisphere. The minimum of 6 DU can be found in January, the maximum of 29 DU in October. While the index ranges from 6 DU to 10 DU from January

to July, we observe an increase from July to October and again a sharp decrease until December. This emphasises that the vortex displacement is clearly evident in wave number one.

We now discuss the differences in hemispheric ozone variability index one between E2000 and T2000 (Fig. 6). The findings of the detailed latitudinal analysis (Fig. 5) are well reflected and summarized in the hemispheric diagnostics. In the Northern Hemisphere strong wave activity in winter and spring accompanied by ozone accumulation leads to high amplitudes of wave number one in the ozone field. The overall coincidence of E2000 and T2000 is well in the Northern Hemisphere, except for the winter months. To quantify the differences, E2000 overestimates the amplitudes in wave one significantly from October to March by 21% to 55%. Besides a too strong wave one activity, this could further indicate that the transition to the winter circulation is mostly too fast and the mean winter circulation itself in spring too persistent. Concerning the interannual variability, E39/C shows a too strong variability in all month months except for March to May. The overestimation is highest during winter.

In the Southern Hemisphere the off-pole displacement of the polar vortex and the depth of the ozone hole strongly contribute to the signal. While model and observations coincide well in amplitude and their interannual variability from January to August, despite a negative bias, they start to differ during the ozone hole season. The index one shows too small values by the model during ozone hole season in September (–38%), October (–56%) and November (–25%). The interannual variability of the ozone hole concerning off-pole displacement and depth is underestimated by E2000. An overestimation of the index one in December and January by 52% and 30%, respectively, indicates again the too persistent ozone hole in the model. Thus, also the interannual variability for January is slightly overestimated by E39/C.

4.2.4 Zonal amplitudes of wave two

Supplementary to the behaviour of the amplitude of wave one, we discuss wave number two in the following section (Fig. 7). The latitudinal distribution for each month is to

some extent similar to the behaviour of the wave one amplitudes in Fig. 5 (note the different range of the ordinate). For both data sets, T2000 and E2000, small amplitudes can be found in the tropics throughout the year. Maximum values in the Northern Hemisphere of about 20 DU to 26 DU occur from January to March at 60° N. In the Southern Hemisphere maxima of 12 DU to 15 DU can be found from September to November at 60° S. Despite some exceptions, E2000 matches the statistical moments of the zonal amplitudes as function of latitude well. The latitudinal position of the maxima is met in each month. A very good coincidence is obvious for the steep gradients in the amplitudes in the Northern Hemisphere between 40° and 50°, especially in January and December. From January to May model and observations fit well in the tropics and subtropics. From June to September E2000 forms a relative maximum shifting from 10° N to 10° S which is not evident in the observations.

In the Southern Hemisphere E2000 shows a pronounced relative maximum at 30° to 40° N from June to August. Since this relative maximum is not that distinct in T2000, mean and standard deviation are overestimated by far by the model. The amplitudes are generally overestimated in the Southern Hemisphere from July to September, but show too small values in October and November. In November at 65° S E2000 underestimates the amplitudes by a factor of 3.5. In December the deviation is not significant anymore. To summarize, the signature of wave number two in the total ozone fields is too weak during the ozone hole season. Especially in October and November a strong wave two contribution characterises vortex elongation and erosion, which eventually leads to the final warming.

4.2.5 Hemispheric ozone variability index two

The diagnostics for both hemispheres allows a generalisation of the findings. Therefore, we compare the hemispheric ozone variability index two of the data sets E2000 and T2000. The T2000 values were already discussed in Fig. 2 (bottom) for all TOMS Version 8 observations from 1978 to 2004. For comparison reasons to E2000 the observations are in the following confined to the period 1996 to 2004 (Fig. 8). Nev-

ertheless, the statistical moments for wave two and their annual cycle are similar for both periods. Since trend analysis is not a subject of this study the differences are not discussed taking into account significance.

As can be inferred from T2000, the annual cycle of the hemispheric ozone variability index two for the Northern Hemisphere shows the maximum of 11 DU in January and the minimum of 4.5 DU occurring in September. In the Southern Hemisphere the index shows a relatively smooth behaviour with an annual amplitude range of 3 DU only. A weak increase from January (3 DU) to November (6 DU) can be detected, followed by a decrease in December to 3.5 DU. When comparing T2000 with respect to E2000 we find for the Northern Hemisphere a significant overestimation of up to 44% in the summer (June to August). For the rest of the year E39/C performs quite well. Even the year-to-year variability is matched from October to December.

For the Southern Hemisphere the picture is different. The deviations are contrary to those for the hemispheric ozone variability index one. Concerning index two we find an overestimation from July to September peaking in 61% in August, and an underestimation of 55% in November.

5 Discussion and Conclusion

In this study global total column ozone observations from TOMS were used to quantify the zonal and hemispheric variability of the lower and middle stratosphere. A spectral statistical Harmonic Analysis is applied to derive amplitudes and phases of the zonal waves number one and two. Total ozone proves to be a valuable coupled dynamical and chemical tracer. Hence, the resulting parameters can be interpreted to a large extent as a representation of the quasi-stationary planetary waves number one and two considering also variability caused by chemical processes. We finally present a diagnostic that enables to analyse the resulting hemispheric variability.

In a first step, the diagnostics was applied to all TOMS total ozone observations (Version 8.0) from November 1978 to October 2004 on a monthly mean basis. The time

series of the ozone variability index one is dominated by a pronounced annual cycle with maxima during winter and minima during summer. The clear anti-correlation of the index in both hemispheres is interpreted as a lack of planetary wave activity during the summer months. In the Southern Hemisphere the largest hemispheric ozone variability indices one are associated to off-pole displacements of the polar vortex. Since the index is a coupled dynamical and chemical parameter it reflects also the increased amplitudes in the zonal ozone field due to reduced ozone levels inside the vortex. Increased indices two indicate an elongation of the polar vortex.

In a second step the diagnostic is exemplified with results of the coupled-chemistry climate model ECHAM4.L39(DLR)/CHEM (E39/C). Total ozone results from a time slice experiment carried out under year 2000 conditions and corresponding TOMS total ozone observations from October 1996 to 2004 are considered. TOMS provides a consistent, measured data set of total ozone with proven accuracy. It is further not influenced by systematic errors due to modelling, assimilation or meteorological analyses. Thus, it provides an excellent reference data set for our analysis.

Concerning the hemispheric total ozone budget, E39/C shows a positive bias up to 18.2% in the Northern and up to 11.4% in the Southern Hemisphere. The inter- and intra-annual variability is well met; especially in the Northern Hemisphere the absolute bias is nearly constant throughout the year. The model improvements have reduced the positive total ozone bias at southern polar latitudes only.

Summarizing the main differences of E2000 and T2000 for the hemispheric ozone variability indices, we conclude that both indices, one and two, are preferably too high in the Northern Hemisphere and preferably too low in the Southern Hemisphere. Further, it can not be followed that positive or negative deviations of the indices one and two are clearly anticorrelated to the respective deviations in the other hemisphere related to the annual cycle.

The overall coincidence is better in the Northern Hemisphere. However, we identify a strong overestimation of index one for the winter months. Additionally, the interannual variability is too strong in all months except for spring. We infer that in the North-

ern Hemisphere E39/C produces a too strong planetary wave one activity in winter and spring accompanied by a too strong polar vortex. Comparing mean and standard deviation of the hemispheric ozone variability index two for all month we find for the Northern Hemisphere a significant overestimation of up to 44% in the summer. For the remainder of the year E39/C performs well.

For the Southern Hemisphere we conclude that model and observations differ significantly during the ozone hole season concerning wave one and two. As the amplitudes of both, wave number one and two, are underestimated in September and October E39/C exhibits a too stable and strong polar vortex. Consequently, this explains the too low interannual variability of the ozone hole. The diagnostic further revealed a strong negative bias of wave number one amplitudes in the tropics and subtropics from October to December which may also contribute to the zonal-symmetric polar vortex. The general underestimation of the indices for the Southern Hemisphere coincides with the cold bias. On the contrary, we identify an overestimation of the index one in December and January up to 52%. This indicates a too persistent ozone hole in the model.

Unlike hemispheric ozone variability index one, index two shows positive deviations in the Southern Hemisphere from July to September (up to 61% in August), negative deviations by 55% in November. The lack of wave two variability in October and November leads to weak vortex elongation, erosion and eventually a too late final warming. The too high wave number two amplitudes in July and August might cause a too strong meridional heat flux and contribute to the problem that the polar vortex is formed too late in season.

Since the ozone zonal mean values for the ozone hole coincide well in October we link the differences to dynamics. Concerning the forcing of wave one and two the representation of sea surface temperatures and ice coverage should be inspected and sensitivity studies performed. The impact of interannual variations of sea surface temperatures on stratospheric dynamics and ozone was shown by Braesicke and Pyle (2004). Additionally, the underestimation of wave one might be attributed to the underestimation of the orography of the Andes. Thus, their orographic representation should

be improved and its sensitivity studied.

Since the diagnostic is applied on a monthly basis it further allows identifying suspicious months on a global scale for more detailed studies: e.g. the hemispheric mean of wave number two shows significantly too high values in July for both hemispheres. The same is the case for the hemispheric mean wave number one in December.

It has to be emphasized that E39/C reproduces smaller scale structures like relative minima in zonal amplitudes in the tropics and subtropics mainly well. The link between large scale wave activity and the quantitative representation of meridional transport, especially for subtropical-mixing into the mid-latitudes in E39/C needs further investigation (Eyring et al., 2003) with respect to the applied transport scheme.

We conclude that the simple hemispheric diagnostics with its robust quantities gains reliable results in order to quantify model-observation differences. As a main advantage the diagnostic summarizes dynamics and chemistry in one parameter that can easily be derived on a monthly basis. Although a period of only eight years is chosen (TOMS data from 1996 to 2004), it proved to be representative on a hemispherical scale. The robust diagnostic is not sensitive to outliers and is therefore also suited for trend analysis. If the diagnostics is confined to wave numbers one and two in the total ozone field it will result in true climatological (mean) features, while for wave number three and higher the interannual variation is of the same order than the average. In this study the diagnostic is applied to results of a time slice experiment for fixed climate conditions that gains different representations of a year. Time series of the hemispheric ozone variability indices can further be applied to evaluate results of transient runs of CCMs (e.g. Dameris et al., 2005).

In general, the hemispheric ozone variability indices can be regarded as a simple and robust approach to evaluate differences in total ozone variation of different CCMs. Therefore, the diagnostic is recommended as core diagnostic for model intercomparisons by the CCM Validation Activity for SPARC (Eyring et al., 2005).

Furthermore, satellite borne instruments to monitor the global total ozone variability with proven accuracy like the upcoming GOME-2 on METOP are required to set up a

long-term perspective of this work. This is of special concern for continuously improving coupled-chemistry climate model evaluation and for tracing signs of recovery of the ozone layer and the Antarctic ozone hole in particular.

Acknowledgements. The Ozone Processing Team of NASA is kindly acknowledged for the TOMS data.

References

Andrews, D. G., Holton J. R., and Leovy, C. B.: Middle Atmosphere Dynamics, Academic Press, Inc, Orlando, USA, 1987.

Appenzeller, C., Weiss, A. K., and Staehelin, J.: North Atlantic Oscillation modulates total ozone winter trends, Geophys. Res. Lett., 27, 1134–1138, 2000.

Austin, J., Shindell, D., Beagley, S. R., Brühl, C., Dameris, M., Manzini, E., Nagashima, T., Newman, P., Pawson, S., Pitari, G., Rozanov, E., Schnadt, C., and Shepherd, T. G.: Uncertainties and assessments of chemistry-climate models of the stratosphere, Atmos. Chem. Phys., 3, 1–27, 2003.

Barnett, J. J. and Labitzke, K.: Climatological distribution of planetary waves in the middle atmosphere, Adv. Space Res., 10, 63–91, 1990.

Benkovitz, C. M., Scholtz, M. T., Pacyna, J., Tarrason, L., Dignon, J., Voldner, E. C., Spiro, P. A., Logan, J. A., and Graedel, T. E.: Global gridded inventories of anthropogenic emissions of sulphur and nitrogen, J. Geophys. Res., 101, 29 239–29 253, 1996.

Bhartia, P. K. and Wellemeyer, C.: TOMS version 8 Algorithm Theoretical Basis Document, http://toms.gsfc.nasa.gov, November 24, 2004.

Bittner, M., Offermann, D., Bugaeva, I. V., et al.: Long period/large scale oscillations of temperature during the DYANA campaign, J. Atmos. Terr. Phys., 56, 1675–1700, 1994.

Bittner, M., Dech, S., and Loyola D.: Planetary scale waves in total ozone from ERS-2 GOME, ESA SP-414, 703–706, 1997.

Bojkov, R. D. and Fioletov, V. E.: Estimating the global ozone characteristics during the last 30 years, J. Geophys. Res., 100, 16 537–16 551, 1995.

Bojkov, R. D. and Balis, D. S.: Characteristics of episodes with extremely low ozone values in the northern middle latitudes 1957-2000, Ann. Geophys. 19, 797–807, 2001.

Braesicke, P. and Pyle, J. A.: Sensitivity of dynamics and ozone to different representations of SSTs in the Unified Model, Q. J. R. Meteorol. Soc., 99, 1–9, 2004.
Charney, J. G. and Drazin, P. G.: Propagation of planetary-scale disturbances from the lower atmosphere into the upper atmosphere, J. Geophys. Res., 66, 83–109, 1961.
Dameris, M., Nodorp, D., and Sausen, R.: Correlation between tropopause height, pressure and TOMS data for the EASOE-winter 1991/1992, Beitr. Phys. Atmosph., 68, 227–232, 1995.
Dameris, M., Grewe, V., Ponater, M., Deckert, R., Eyring, V., Mager, F., Matthes, S., Schnadt, C., Stenke, A., Steil, B., Brühl, C., and Giorgetta, M. A.: Long-term changes and variability in a transient simulation with a chemistry-climate model employing realistic forcing, Atmos. Chem. Phys., 5, 2121–2145, 2005.
Dameris, M., Matthes, S., Deckert, R., Grewe, V., and Ponater, M.: Solar cycle effect delays onset of ozone recovery, Geophys. Res. Lett., 33, L03806, doi:10.1029/2005GL024741, 2006.
Dobson, G. M. B. and Harrison, D. N.: Measurements of the amount of ozone in the earth's atmosphere and its relation to other geophysical conditions, Proc. Roy. Soc. London, A 110, 660–693, 1926.
Eyring, V., Dameris, M., Grewe, V., Langbein, I., and Kouker, W.: Climatologies of subtropical mixing derived from 3D models, Atmos. Chem. Phys., 3, 1007–1021, 2003.
Eyring, V., Harris, N. R. P., Rex, M., Shepherd, T. G., Fahey, D. W., Amanatidis, G. T., Austin, J., Chipperfield, M. P., Dameris, M., De, P. M., Forster, F., Gettelman, A., Graf, H.-F., Nagashima, T., Newman, P. A., Pawson, S., Prather, M. J., Pyle J. A., Salawitch R. J., Santer, B. D., and Waugh, D. W.: A strategy for process-oriented validation of coupled chemistry-climate models, Bull. Am. Meteorol. Soc., 86, 1117–1133, 2005.
Giorgetta, M. A., Manzini, E., and Roeckner, E.: Forcing of the quasi-biennial oscillation from a broad spectrum of atmospheric waves, Geophys. Res. Lett., 29, doi:10.1029/2002GL014756, 2002.
Grewe, V., Brunner, D., Dameris, M., Grenfell, J. L., Hein, R., Shindell, D., and Staehelin, J.: Origin and variability of upper tropospheric nitrogen oxides and ozone at northern mid-latitudes, Atmos. Environ., 35, 3421–3433, 2001.
Grewe, V., Dameris, M., Fichter, C., and Sausen, R.: Impact of aircraft NOx emissions. Part 1: interactively coupled climate-chemistry simulations and sensitivities to climate-chemistry feedback, lightning and model resolution, Meteorol. Z., 11, 177–186, 2002.
Haigh, J.: The impact of solar variability on climate, Science, 272, 981–984, 1996.

Hao, W. M., Liu, M.-H., and Crutzen, P. J.: Estimates of annual and regional releases of CO and other trace gases to the atmosphere from fires in the tropics, based on the FAO statistics for the period 1975–1980, in: Fire in the Tropical Biota, Ecological Studies 84, edited by: Goldammer, J. G., Springer-Verlag, New York, USA, 440–462, 1990.

Hadjinicolaou, P., Pyle, J. A., and Harris, N. R. P.: The recent turnaround in stratospheric ozone over northern middle latitudes: A dynamical modeling perspective, Geophys. Res. Lett., 32, L12821, doi:10.1029/2005GL022476, 2005.

Hein, R., Dameris, M., Schnadt, C., Land, C., Grewe, V., Köhler, I., Ponater, M., Sausen, R., Steil, B., Landgraf, J., and Brühl, C.: Results of an interactively coupled atmospheric chemistry-general circulation model: Comparison with observations, Ann. Geophys., 19, 435–457, 2001.

Huck, P. E., McDonald, A. J., Bodeker, G. E., and Struthers, H.: Interannual variability in Antarctic ozone depletion controlled by planetary waves and polar temperatures, Geophys. Res. Lett., 32, L13819, doi:10.1029/2005GL022943, 2005.

IPCC: Climate Change 2001, The Scientific Basis, Contribution of Working Group I to the Third Assessment Report of the Intergovernmental Panel on Climate Change, edited by: Houghton, J. T., Ding, Y., Griggs, D. J., Noguer, A., van der Linden, P. J., Dai, X., Maskell, K., and Johnson, C. A., Cambridge University Press, 2001.

IPCC/TEAP (Intergovernmental Panel on Climate Change/Technology and Economic Assessment Panel), Special report on safeguarding the ozone layer and the global climate system: Issues related to hydrofluorocarbons and perfluorocarbons, prepared by working group I and III od IPCC/TEAP, edited by: Metz, B., Jager de, D., Kuijpers, L., et al., Cambridge University Press, Cambridge, United Kingdom and New York, NY, USA, 488pp., 2005.

James, P. M.: A climatology of ozone mini-holes over the Northern Hemisphere, Int. J. Climatol., 18, 1287–1303, 1998.

Kayano, M. T.: Principal modes of total ozone on the Southern Oscillation timescale and related temperature variations, J. Geophys. Res., 102, 25 797–25 806, 1997.

Labitzke, K., Austin, J., Butchart, N., Knight, J., Takahashi, M., Nakamoto, M., Nagashima, T., Haigh, J., and Williams, V.: The global signal of the 11-year solar cycle in the stratosphere: observations and models, J. Atmos. Solar-Terr. Phys., 64, 203–210, 2002.

Lamago, D., Dameris, M., Schnadt, C., Eyring, V., and Brühl, C.: Impact of large solar zenith angles on lower stratospheric dynamical and chemical processes in a coupled chemistry-climate model, Atmos. Chem. Phys., 3, 1981–1990, 2003.

Land, C., Feichter, J., and Sausen, R.: Impact of vertical resolution on the transport of passive tracers in the ECHAM4 model, Tellus, 54B, 344–360, 2002.
Newchurch, M. J., Yang E.-S., Cunnold, D. M., Reinsel, G. C., Zawodny, J. M., and Russell III, J. M.: Evidence for slowdown in stratospheric ozone loss: First stage of ozone recovery, J. Geophys. Res., 108, 4507, doi:10.1029/2003JD003471, 2003.
Newman, P. A. and Schoeberl, M. R.: October Antarctic Temperature and Total Ozone Trends from 1979–1985, Geophys. Res. Lett., 13, 1206–1209, 1986.
Nikulin, G. N. and Repinskaya, R. P.: Modulation of total ozone anomalies in the midlatitude Northern Hemisphere by the arctic oscillation, Izvestiya, Atm. Oceanic Phys., 37(5), 633–643, 2001.
Ortega, J. and Rheinboldt, W.: Iterative solution of nonlinear equations in several variables, New York, Academic Press, 1970.
Rayner, N. A., Parker, D. E., Horton, E. B., Folland, C. K., Alexander, L. V., Rowell, D. P., Kent, E. C., and Kaplan, A.: Global analyses of sea surface temperatures, sea ice, and nightmarine air temperature since the late nineteenth century, J. Geophys. Res., 108, 4407, doi:10.1029/2002JD002670, 2003.
Reed, R. J.: The role of vertical motions in ozone-weather relationship, J. Meteor., 7, 263–267, 1950.
Robock, A.: Volcanic eruptions and climate, Rev. Geophys., 38, 191–219, 2000.
Salby, M. L.: Survey of planetary scale travelling waves: The state of theory and observations, Rev. Geophys. Space Phys., 22, 209–236, 1984.
Sander, S. P., Friedl, R. R., DeMore, W. B., et al.: Chemical Kinetics and Photochemical Data for Use in Stratospheric Modeling, JPL Publication 00-3, NASA Jet Propulsion Laboratory, 2000.
Schoeberl, M. R., Krueger, A. J., and Newman, P. A.: The Morphology of Antarctic Total Ozone as seen by TOMS, Geophys. Res. Lett., 13, 1217–1220, 1986.
Schoeberl, M. R. and Hartmann, D. L.: The dynamics of the stratospheric polar vortex and its relation to springtime ozone depletions, Science, 251, 46–52, 1991.
Schnadt, C. and Dameris, M.: Relationship between North Atlantic Oscillation changes and stratospheric ozone recovery in the Northern Hemisphere in a chemistry-climate model, Geophys. Res. Lett., 30, doi:10.1029/2003GL017006, 2003.
Schnadt, C., Dameris, M., Ponater, M., Hein, R., Grewe, V., and Steil, B.: Interaction of atmospheric chemistry and climate and its impact on stratospheric ozone, Clim. Dynamics, 18,

501–517, 2002.
SPARC/IOC/GAW: Assessments of Trends in the Vertical Distribution of Ozone, SPARC Report No 1, http://www.aero.jussieu.fr/~sparc/SPARCReport1/, 1998.
Steil, B., Dameris, M., Brühl, C., Crutzen, P. J., Grewe, V., Ponater, M., and Sausen, R.: Development of a Chemistry Module for CGMs: first results of a multi-year integration, Ann. Geophys., 16, 205–228, 1998.
Steil, B., Brühl, C., Manzini, E., Crutzen, P. J., Lelieveld, J., Rasch, P. J., Roeckner, E., and Krueger, K.: A new interactive chemistry-climate model. 1. Present day climatology and interannual variability of the middle atmosphere using the model and 9 years of HALOE/UARS data, J. Geophys. Res., 108, doi:10.1029/2002JD002971, 2003.
Steinbrecht, W., Hassler, B., Claude, H., Winkler, P., and Stolarski, R. S.: Global distribution of total ozone and lower stratospheric temperature variations, Atmos. Chem. Phys., 3, 1421–1438, 2003.
Steinbrecht, W., Claude, H., Köhler, U., and Winkler, P.: Interannual changes of total ozone and Northern Hemisphere circulation patterns, Geophys. Res. Lett., 28, 1191–1194, 2001.
Steinbrecht, W., Claude, H., and Winkler, P.: Enhanced upper stratospheric ozone: Sign of recovery or solar cycle effect?, J. Geophys. Res., 109, doi:10.1029/2003JD004284, 2004.
Steinbrecht, W. , Haßler, B., Brühl, C., Dameris, M., Giorgetta, M. A., Grewe, V., Manzini, E., Matthes, S., Schnadt, C., Steil, B., and Winkler, P.: Interannual variation patterns of total ozone and lower stratospheric temperature in observations and model simulations, Atmos. Chem. Phys., 6, 349–374, 2006.
Stolarski, R. S., Krueger, A. J., Schoeberl, M. R., McPeters, R. D., Newman, P. A., and Alpart, J. C.: NIMBUS 7 SBUV/TOMS measurements of the springtime Antarctic ozone hole, Nature, 322, 808–814, 1986.
Thomas, W., Baier, F., Erbertseder, T., and Kästner, M.: The Algeria severe weather event of November 1999 and its impact on ozone and NO2 distributions, Tellus B, 55(5), 993–1006, 2003.
Turco, R. P., Toon, O. B., and Hamill, P.: Heterogeneous physiochemistry of the polar ozone hole, J. Geophys. Res., 94, 16 493–16 510, 1989.
Wirth, V.: Quasi-stationary planetary waves in total ozone and their correlation with lower stratosphere temperature, J. Geophys. Res., 98, 8873–8882, 1993.
World Meteorological Organisation: Scientific Assessment of Ozone Depletion: 1998 Global Ozone Research and Monitoring, Report No 44, Geneva, 1999.

World Meteorological Organisation: Scientific Assessment of Ozone Depletion: 2002 Global Research and Monitoring Project, Report No 47, Geneva, 2003.

Yang, E.-S., Cunnold, D. M., Newchurch, M. J., and Salawitch, R. J.: Change in ozone trends at southern high latitudes, Geophys. Res. Lett., 32, L12812, doi:10.1029/2004GL022296, 2005.

Yienger, J. J. and Levy II, H.: Empirical model of global soil-biogenic NOx emissions, J. Geophys. Res., 100, 11 447–11 464, 1995.

Zerefos, C. S., Bais, A., Ziomas, I. C., and Bojkov, B. R.: One the relative importance of Quasi-Biennial Oscillation and El Nino Southern Oscillation in the revised Dobson Total Ozone records, J. Geophys. Res., 100, 10 135–10 144, 1992.

Zerefos, C. S., Tourpali, K., Bojkov, B. R., Balis, D., Rognerund, B., and Isaksen, I. S. A.: Solar activity – total column ozone relationships: observations and model studies with heterogeneous chemistry, J. Geophys. Res., 102, 1561–1569, 1997.

Table 1. Driving Parameters for the E39/C time-slice experiment under "2000" conditions.

		2000	Reference
CO_2	[ppmv]	376	IPCC (2001)
CH_4	[ppmv]	1.76	IPCC (2001)
N_2O	[ppbv]	316	IPCC (2001)
Cl_y	[ppbv]	3.4	WMO (1999)
NO_x lightning	(Tg(N)/year)	5.0	Grewe et al. (2001)
NO_x air traffic	(Tg(N)/year)	0.7	Schmidt and Brunner (1997)
NO_x surface (industry, traffic)	(Tg(N)/year)	33.0	Benkovitz et al. (1996)
NO_x surface (soils)	(Tg(N)/year)	5.6	Yienger and Levy (1995)
NO_x surface (biomass burning)	(Tg(N)/year)	7.0	Hao et al. (1990)

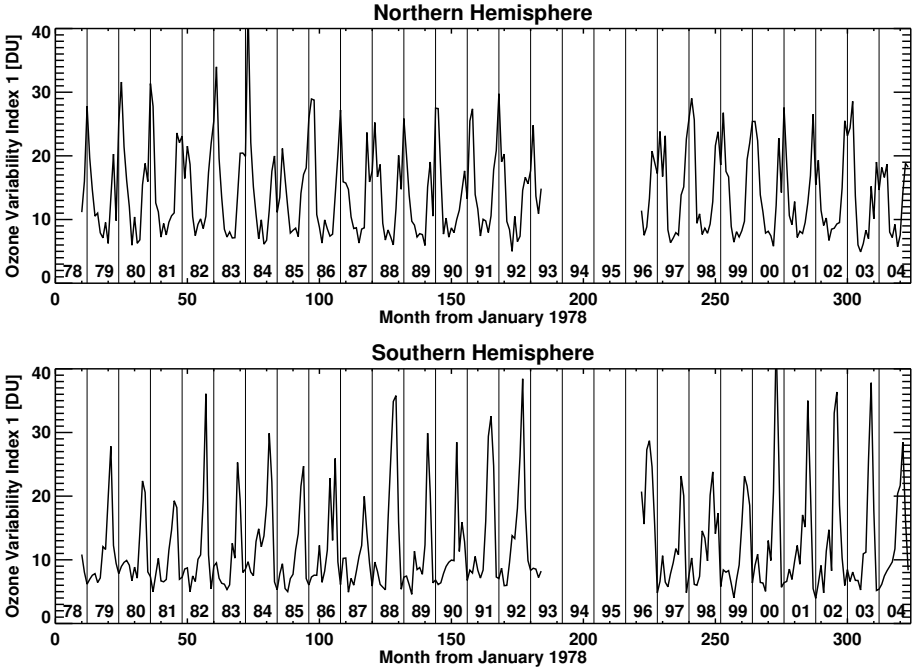

Fig. 1. Time series of the monthly mean hemispheric ozone variability index number one derived from TOMS total ozone observations from 1978 to 2004 for the Northern (top) and Southern Hemisphere (bottom). Only TOMS data of version 8.0 is used. Thus, TOMS on METEOR is not considered.

ACPD
6, 5671–5709, 2006

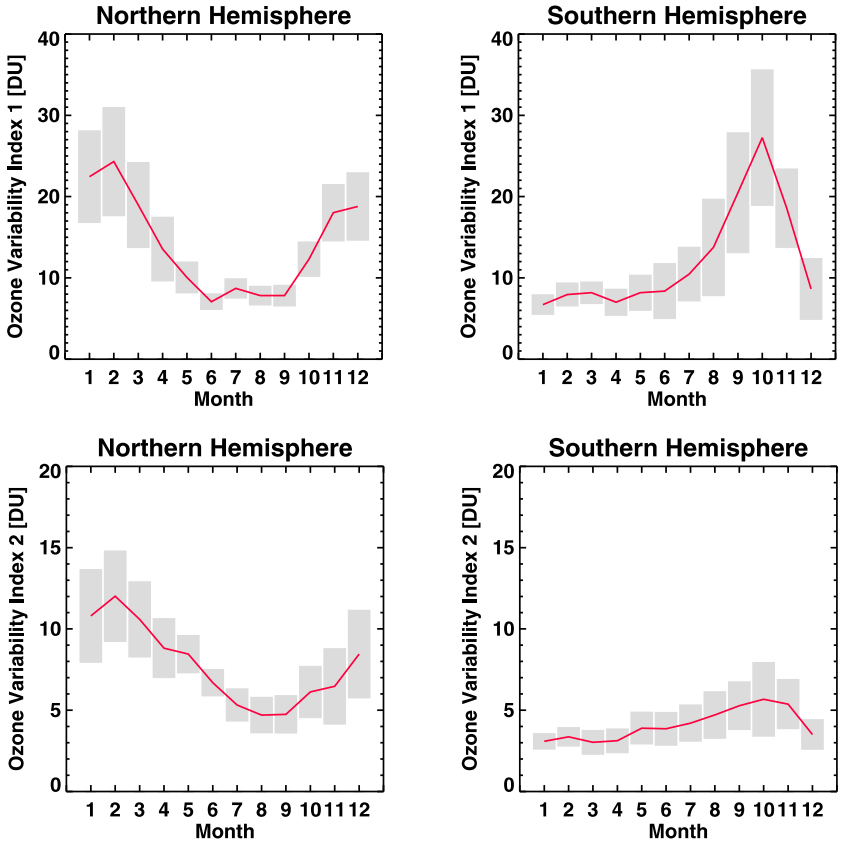

Fig. 2. Interannual mean and standard deviation of the hemispheric ozone variability index one (top) and two (bottom) for each month (Northern Hemisphere left; Southern Hemisphere right). The results are derived for all available TOMS total ozone observations (Version 8) between November 1978 and October 2004. Note the different scale of the y-axis for indices one and two. The grey bars indicate the standard deviation.

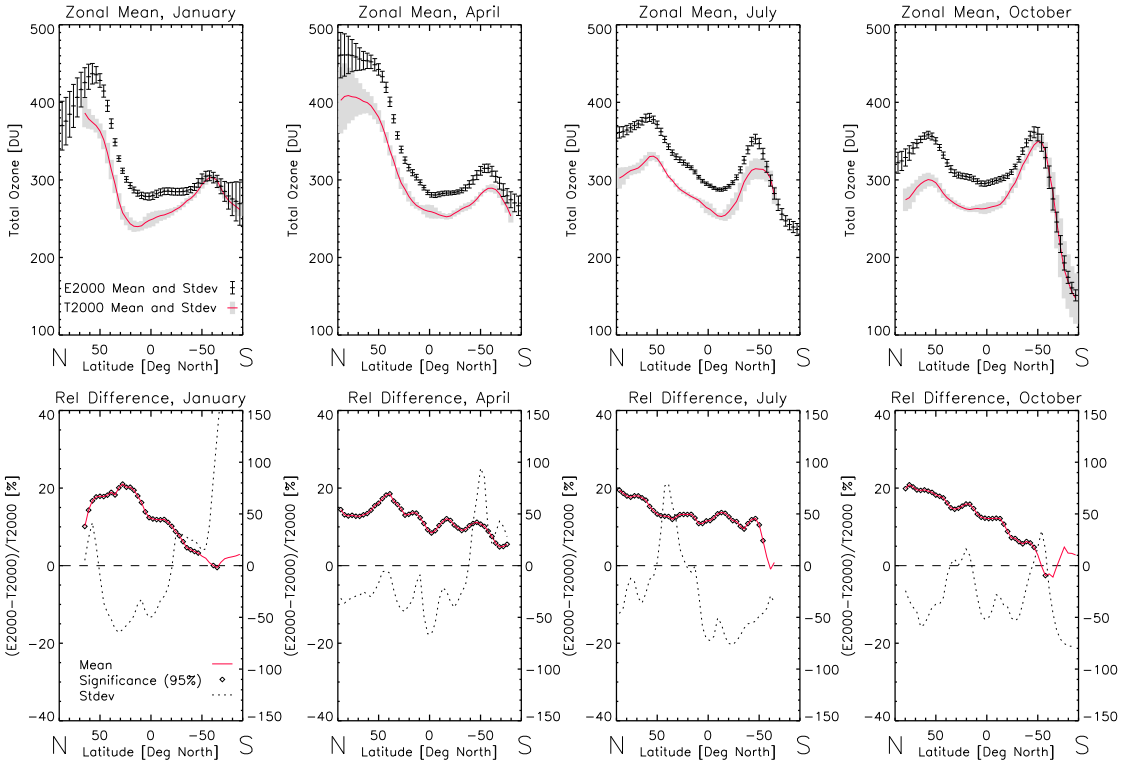

Fig. 3. Zonal means of total ozone for January, April, July and October (top). 20 years of the E39/C time slice experiment "2000" (E2000) are compared to corresponding TOMS data (T2000). E2000 is represented by bars in black (mean and standard deviation), T2000 by the solid (red) curve and grey bars (mean and standard deviation). Below the corresponding relative differences of means (left y-axis) and standard deviations (right y-axis) are denoted. A diamond indicates statistical significance for the relative difference of the mean at the 95% level.

ACPD
6, 5671–5709, 2006

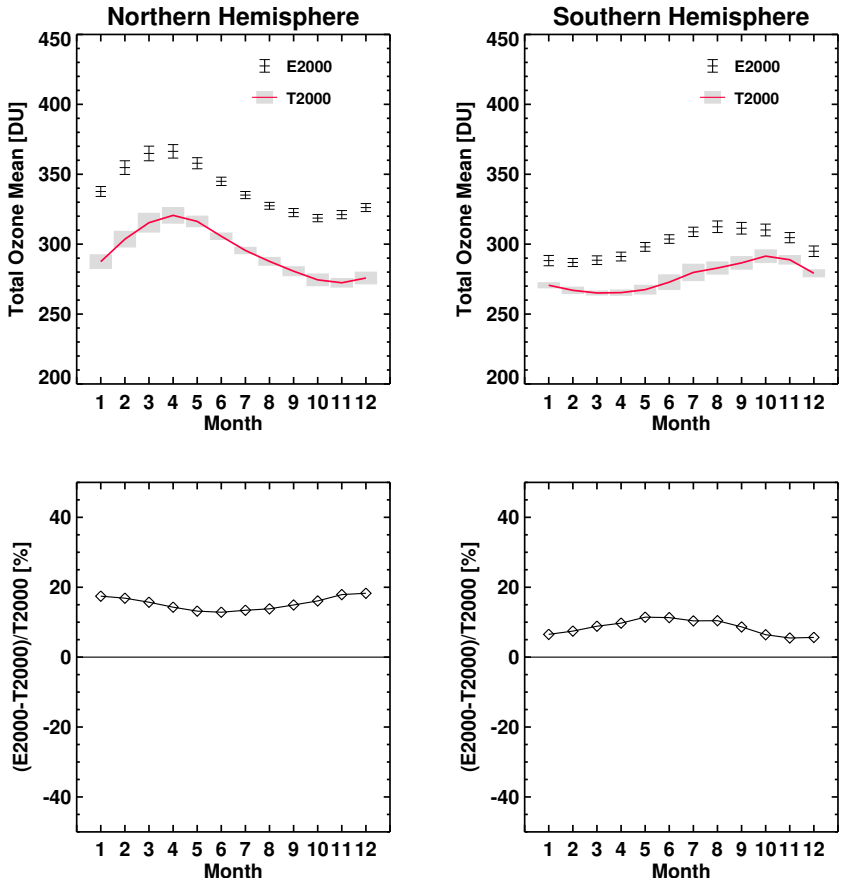

Fig. 4. Hemispheric monthly means of total ozone for E2000 and T2000 (Northern Hemisphere left, Southern Hemisphere right). Mean and standard deviation for E2000 is depicted by bars in black, T2000 mean by a solid (red) line with grey bars indicating the standard deviation (top). Below the corresponding relative differences are shown. Diamonds denote significance at the 95% significance level.

ACPD
6, 5671–5709, 2006

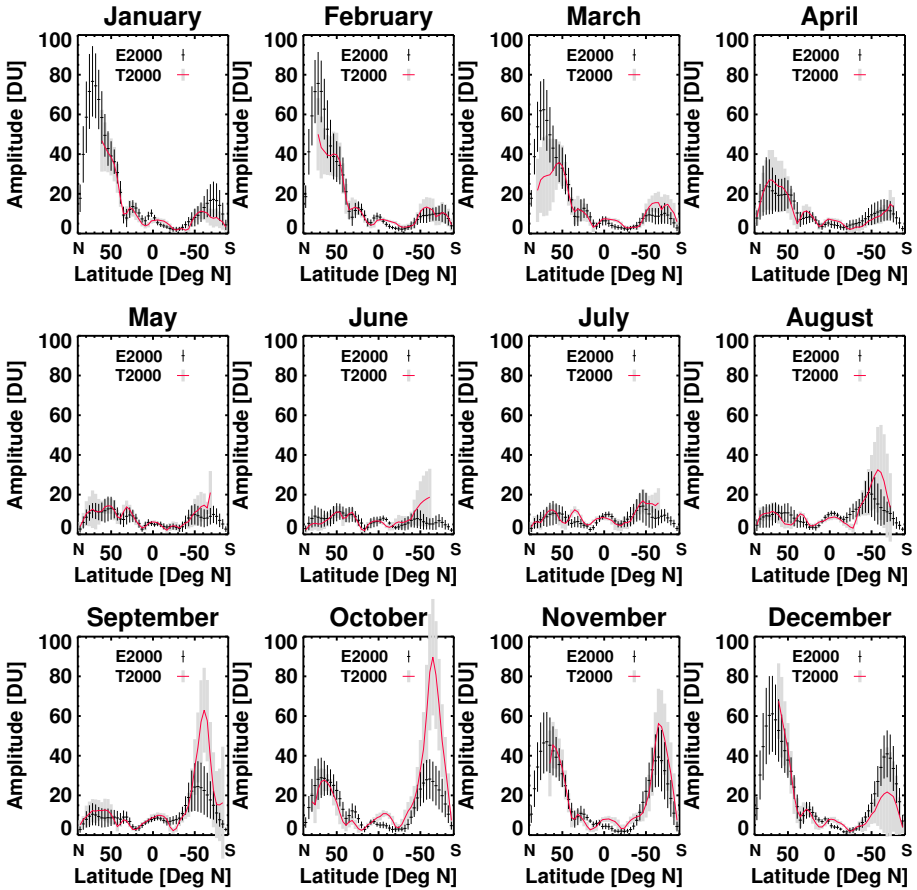

Fig. 5. Zonal amplitudes of wave number one as a function of latitude for each month for E2000 and T2000. Mean and standard deviation are indicated by black bars for E2000 and by the solid (red) curve and grey bars for T2000.

ACPD
6, 5671–5709, 2006

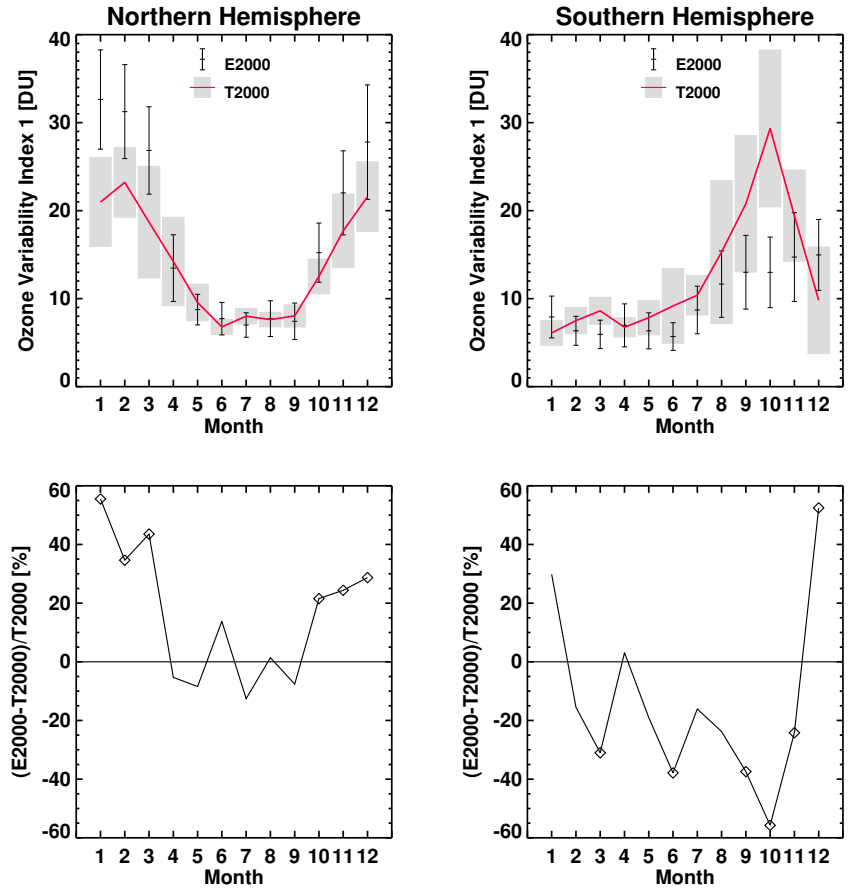

Fig. 6. Hemispheric ozone variability index one for each month covering the years of E2000 and T2000 (Northern Hemisphere left, Southern Hemisphere right). Mean and standard deviation are indicated by black bars for E2000 and by the solid (red) curve and grey bars for T2000 (top). Below the corresponding relative differences are depicted. The diamond symbols indicate statistical significance at the 95% level.

ACPD
6, 5671–5709, 2006

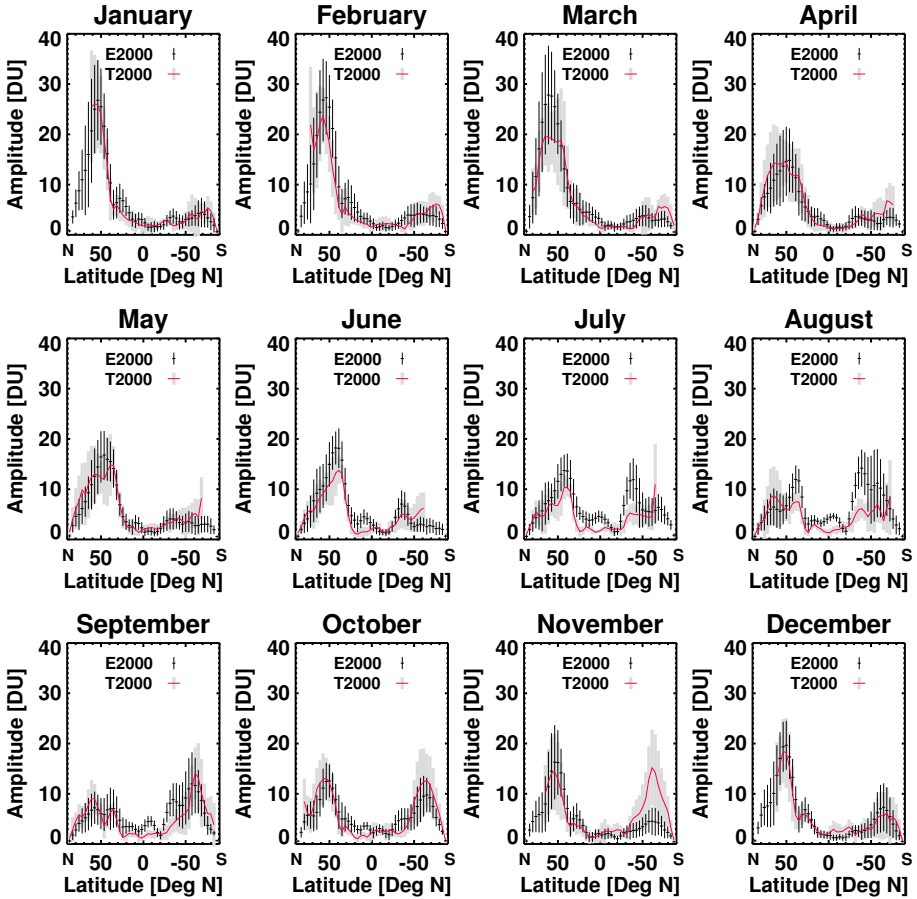

Fig. 7. Zonal amplitudes of wave number two as traced by the total ozone field as a function of latitude for each month for E2000 and T2000. Mean and standard deviation are indicated by black bars for E2000 and by the solid (red) curve and grey bars for T2000.

ACPD
6, 5671–5709, 2006

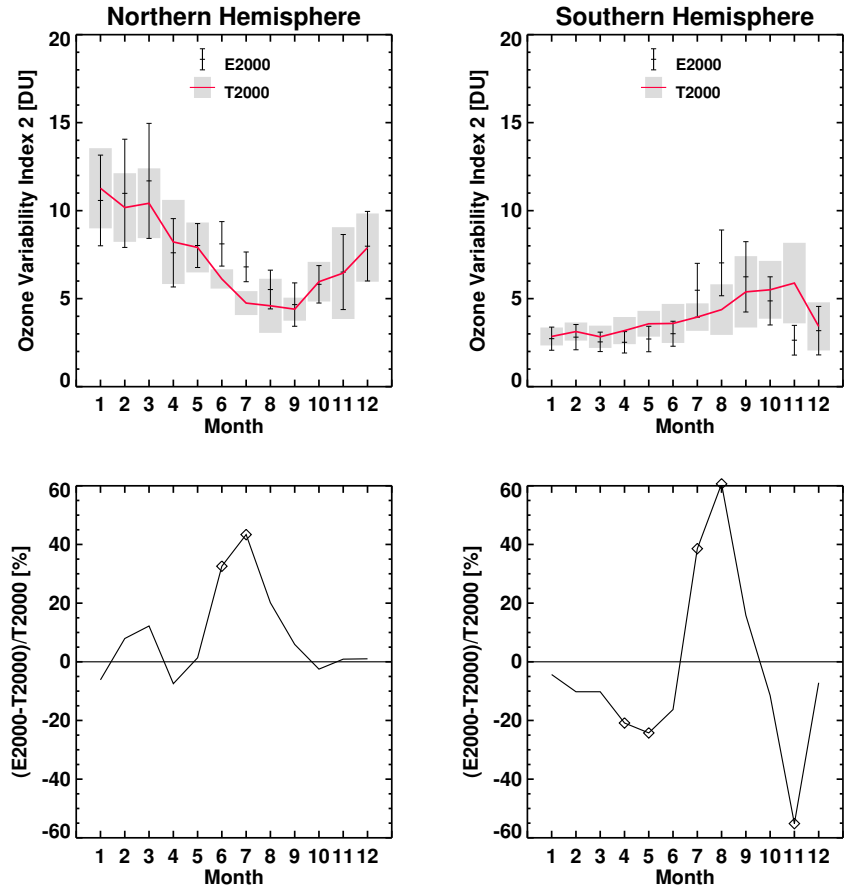

Fig. 8. Hemispheric ozone variability index 2 for each month covering the years E2000 and T2000 (Northern Hemisphere left, Southern Hemisphere right). Mean and standard deviation are indicated by black bars for E2000 and by the solid (red) curve and grey bars for T2000 (top). Below the corresponding relative differences are denoted. The diamond symbols indicate statistical significance at the 95% level.

ACPD
6, 5671–5709, 2006